Thermochimica Acta, 165 (1990) 57–72
Elsevier Science Publishers B.V., Amsterdam

THERMAL EXPANSION OF HYDROXYAPATITE–β-TRICALCIUM PHOSPHATE CERAMICS

SATOSHI NAKAMURA and RYOHEI OTSUKA

Department of Mineral Resources Engineering, School of Science and Engineering, Waseda University, 3-4-1 Okubo, Shinjuku-ku, Tokyo 169 (Japan)

HIDEKI AOKI, MASARU AKAO and NAOKI MIURA

Institute for Medical and Dental Engineering, Tokyo Medical and Dental University, 2-3-10 Kanda-Surugadai, Chiyoda-ku, Tokyo 101 (Japan)

TAKEYUKI YAMAMOTO

Central Research Laboratory, INAX Corporation, Koiehonmachi, Tokoname, Aichi 479 (Japan)

(Received 21 December 1989)

ABSTRACT

The thermal lattice expansion of calcined hydroxyapatite and β-tricalcium phosphate single-phase powder was investigated by high-temperature X-ray diffractometry. The thermal expansion of densely sintered hydroxyapatite–β-tricalcium phosphate composite ceramics was examined by thermomechanical analysis. Hydroxyapatite–β-tricalcium phosphate mixtures with a Ca/P atomic ratio varying from 1.50 to 1.67 were precipitated from $Ca(OH)_2$ and H_3PO_4 solution at room temperature. The powder, calcined in air at 800 ° C for 3 h, was pressed in a mould at 98 MPa. The pressed powder pellets were sintered in air at 1150 ° C for 1 h. High-temperature X-ray powder diffraction data were measured in the temperature range from 25 ° C to 1150 ° C and calibrated by a platinum internal standard technique. Thermomechanical analysis was carried out with a 0.08 kPa compressive load in the range from 25 ° C to 1250 ° C with an α-Al_2O_3 polycrystalline standard. The hydroxyapatite and β-tricalcium phosphate are characterised by non-linear thermal expansion between 25 ° C and 600 ° C because of HPO_4^{2-} condensation and dehydration. In the upper temperature region, the hydroxyapatite c-axial dimension expanded sharply from 1000 ° C to 1150 ° C owing to the formation of oxyapatite. The c-axial dimension of β-tricalcium phosphate shrank from 850 to 950 ° C which was ascribed to the formation of an intermediate phase between the β- and α-tricalcium phosphate phases. The mean (25–1000 ° C) thermal expansion coefficient of the densely sintered hydroxyapatite–β-tricalcium phosphate ceramics increased almost linearly with an increase in β-tricalcium phosphate content.

INTRODUCTION

Hydroxyapatite, $Ca_{10}(PO_4)_6(OH)_2$, is the main inorganic component of vertebrate bone and tooth tissues. β-Tricalcium phosphate, $Ca_3(PO_4)_2$, is similar in chemical and physical properties to hydroxyapatite. Hydroxyapatite and β-tricalcium phosphate ceramics are classified as bioactive materials and combine directly with hard tissues without fibrous connective

0040-6031/90/$03.50

tissues. Sintered hydroxyapatite and β-tricalcium phosphate polycrystalline ceramics have medical applications as bone fillers [1,2], artificial tooth roots [3,4] and percutaneous devices [5]. The low fractural strength and toughness of hydroxyapatite and β-tricalcium phosphate ceramics [6–9] restrict their applications to those devices not requiring a heavy load. For devices requiring a heavy load, hydroxyapatite–β-tricalcium phosphate ceramic-coated stainless steels and titanium alloys have been developed. Although successful results of animal tests and clinical demonstrations for the composite bioactive materials have been reported [10–12], the bonding strength of the interface between the base and the coating layer is insufficient for clinical applications.

A plasma spraying technique is the most effective coating method at present, but it requires high temperature heating of hydroxyapatite–β-tricalcium phosphate. Therefore, a correspondence of thermal coefficient between the metal used as a base and the hydroxyapatite–β-tricalcium phosphate coating over a wide temperature range is necessary for an improvement in the bonding strength.

Hydroxyapatite belongs to the hexagonal system with cell parameters $a = 9.421–9.433$ Å and $c = 6.88$ Å. The a cell parameter variation is attributed to preparation differences and cation impurities, such as CO_3^{2-} and HPO_4^{2-}, and vacancies [13–20]. The thermal lattice expansion data given in the literature [17,20–22] also vary and are limited in temperature to under 1000 ° C. Fine grained (< 0.1 μm) hydroxyapatite prepared for plasma spray coating by a wet method [9] has both HPO_4^{2-} and vacancies. It has been reported by Fischer et al. and Perdok et al. [20,21] that hydroxyapatite with impurities of CO_3^{2-} and HPO_4^{2-}, and vacancies is subject to non-linear thermal expansion.

β-Tricalcium phosphate has a rhombohedral crystal structure with cell parameters of $a = 10.439$ Å and $c = 37.375$ Å (hexagonal setting) [23]. β-Tricalcium phosphate transforms into α-phase in the temperature range 1120–1180 ° C [24]. The thermal expansion data of β-tricalcium phosphate has rarely been reported.

In the present paper, the thermal lattice expansion of hydroxyapatite and β-tricalcium phosphate single-phase powder was investigated by high-temperature X-ray diffractometry. The thermal expansion of densely sintered hydroxyapatite–β-tricalcium phosphate polycrystalline ceramics was also examined by thermomechanical analysis.

EXPERIMENTAL PROCEDURE

Materials

Hydroxyapatite–β-tricalcium phosphate mixtures with a Ca/P atomic ratio varying from 1.50 to 1.67 were precipitated from calcium hydroxide

[$Ca(OH)_2$] and phosphoric acid [H_3PO_4] solution [8]. A 0.5–0.6 M $Ca(OH)_2$ suspension in distilled water was stirred at room temperature and a 0.3–0.4 M H_3PO_4 solution was added slowly, drop-wise. The Ca/P atomic ratios of the products were controlled by the reactant pH which was adjusted by addition of 3% ammonia solution. The gelatinous slurry was filtered and dried at 70 °C for 24 h. Then the products were ground to less than 100 mesh. The hydroxyapatite–β-tricalcium phosphate powder was calcined in air at 800 °C for 3 h.

The calcined powder, with an addition of 3.5% polyvinyl alcohol, was pressed in a mould (diameter 60 mm) at 98 MPa. The pressed powder pellets were sintered in air at 1150 °C for 1 h.

Methods

The Ca/P atomic ratios of the sintered hydroxyapatite–β-tricalcium phosphate ceramics were estimated by quantitative analysis using EDTA back-titration for Ca and the phosphomolybdate technique for P [25]. The phase compositions of the powder were determined by X-ray powder diffractometry. The diffraction data for calculation of the compositions were collected using Ni-filtered Cu $K\alpha$ radiation by measuring hydroxyapatite (300) and β-tricalcium phosphate $(02\overline{1}\overline{0})$ reflection profiles.

The adsorbed and structural CO_3^{2-}, HPO_4^{2-}, $P_2O_7^{4-}$ and H_2O of the hydroxyapatite and β-tricalcium phosphate powder were investigated by IR spectroscopy and TG–DTA. The IR spectra of the powders were examined by a Hitachi 260-50. The sample pellets with KBr were preheated at 105 °C for 1 h. The accuracy of the measurements was ± 2 cm^{-1} in the range from 4000 cm^{-1} to 2000 cm^{-1} and ± 1 cm^{-1} from 2000 cm^{-1} to 250 cm^{-1}. The wavenumbers were calibrated by measuring the polystyrene film spectrum. TG–DTA was carried out on an 810 Thermoflex (Rigaku Co.). The samples were heated up to 1000 °C in air at a rate of 10 °C min^{-1}.

The microstructure of the ceramics was observed with a transmission electron microscope (Hitachi Co., H-800H). The samples were prepared by the argon-ion thinning method.

The lattice constants at 25 °C of both hydroxyapatite and β-tricalcium phosphate single-phase powder were refined by program RLC-3 [26] using the X-ray powder diffraction data. The diffraction data were collected with Ni-filtered Cu $K\alpha$ radiation by precisely measuring the (100), (200), (002), (210), (211), (112), (300), (202), (310), (222) and (213) reflections of hydroxyapatite as well as the (110), $(10\overline{1}\overline{0})$, (214), (128), (220) and $(20\overline{2}\overline{0})$ reflections of β-tricalcium phosphate. Silicon powder (NBS-640) was employed as an internal standard.

The thermal expansion of lattice dimensions for both hydroxyapatite and β-tricalcium phosphate single-phase powder was determined by high-temperature X-ray diffraction data. The high-temperature data were measured with Ni-filtered Cu $K\alpha$ on a PW1700 diffractometer (Philips Co.) equipped with an HTK-10 heating unit (Anton Paar Co.). The reflection profiles were the (002), (211), (112) and (300) peaks of hydroxyapatite and the (214), (300), (128), (110), $(10\bar{1}\bar{0})$ and (220) peaks of β-tricalcium phosphate, with the (111) and (200) peaks of platinum (with purity of 99.99%) as an internal standard. The sample temperature was checked by the transformation point method and found to be accurate to within ±4 °C. The data collection temperatures ranged from 25 °C to 1150 °C and were raised at a rate of 10 °C min^{-1}. The diffraction profile measurements were started after keeping the required temperature constant for 30 min.

The sintering shrinkage of both hydroxyapatite and β-tricalcium phosphate single-phase polycrystalline compacts was measured by thermomechanical analysis on an 814H Thermoflex instrument (Rigaku Co.). The samples were calcined powder, with 3.5% polyvinyl alcohol added, pressed in a mould (diameter 3 mm) at 98 MPa. They were 3 mm (diameter) × 15 mm in size and 53–55% in density measured by the weight method. The compressive load applied to the samples and the α-Al_2O_3 polycrystalline standard [27] was 0.15 kPa. The temperature was increased from room temperature to 1300 °C at a rate of 5 °C min^{-1}.

The thermal expansion of the densely sintered hydroxyapatite–β-tricalcium phosphate polycrystalline ceramics was investigated by thermomechanical analysis. The samples, $3.5 \times 3.5 \times 20\ \text{mm}^3$, were cut from disc-shaped sintered polycrystalline ceramics with a low-speed diamond saw. The

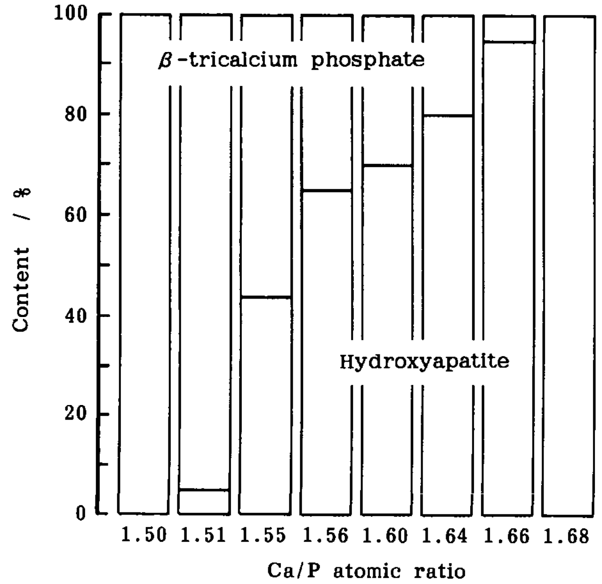

Fig. 1. Phase compositions of hydroxyapatite–β-tricalcium phosphate ceramics sintered at 1150 °C in relation to Ca/P atomic ratios.

compressive load applied to the samples and α-Al_2O_3 polycrystalline standard [27] was 0.08 kPa. The temperature program was three cycles of the sequence: heating in air from 25 °C to 1250 °C at a rate of 5 °C min^{-1}, holding at 1200 °C for 1 h, and then cooling from 1250 °C to 25 °C at a rate of -5 °C min^{-1}.

RESULTS AND DISCUSSION

Phase compositions

The phase compositions of the ceramics sintered at 1150 °C in relation to the Ca/P atomic ratios are shown in Fig. 1. The phase compositions consisted of hydroxyapatite and/or β-tricalcium phosphate. No other phase was detected by X-ray powder diffractometry. A slight absorption of the CO_3^{2-} infrared band at 865, 1413 and 1457 cm^{-1} for hydroxyapatite proved the CO_3^{2-} substitution for PO_4^{3-} [28]. Bands for HPO_4^{2-} at 875 cm^{-1} in both the hydroxyapatite and β-tricalcium phosphate single-phase were clearly visible prior to calcination. After being calcined at 800 °C for 3 h, the HPO_4^{2-} band had almost disappeared, and no $P_2O_7^{4-}$ band was detectable. Although the HPO_4^{2-} condensation reaction [29,30] has been reported as

$$2HPO_4^{2-} \rightarrow P_2O_7^{4-} + H_2O \qquad (1)$$

the disappearance of the $P_2O_7^{4-}$ group suggested that most of the detected HPO_4^{2-} was adsorbed on the surface of the powder. Weight losses of 0.05 and 0.2%, with a broad DTA endotherm at a temperature between 200 and 600 °C were observed for the calcined hydroxyapatite and β-tricalcium phosphate.

The lattice parameters at 25 °C of the calcined β-tricalcium phosphate single-phase powder are shown in Table 1. It has been reported that both *a* and *c* cell parameters increase with an increase in Mg^{2+} content [31]. The measured cell parameters, compared with reported data [23,32], revealed that the β-tricalcium phosphate hardly contained any Mg^{2+}.

TABLE 1

Lattice constants and volume of β-tricalcium phosphate at 25 °C compared with those of β-$Ca_3(PO_4)_2$ and synthetic Mg–whitlockite

	a (Å)	*c* (Å)	*V* (Å^3)
β-Tricalcium phosphate	10.446(2)	37.381	3533(1)
β-$Ca_3(PO_4)_2$ [a]	10.439	37.357	3527
Synthetic Mg–whitlockite [b]	10.350(5)	37.09(1)	3440

[a] B. Dickens et al. [23].

[b] R. Gopal et al. [32].

TABLE 2

Cell dimensions, c/a ratio and percentage expansions, relative to 25 °C, at high temperature for hydroxyapatite

Temperature (°C)	a (Å)	c (Å)	c/a	$\Delta a/a$ (%)	$\Delta c/c$ (%)
25	9.422(2)	6.883(1)	0.7306		
100	9.424(3)	6.883(3)	0.7304	0.021	0.000
150	9.434(4)	6.889(4)	0.7302	0.127	0.087
200	9.436(2)	6.894(2)	0.7306	0.149	0.160
300	9.460(4)	6.910(5)	0.7305	0.403	0.392
400	9.480(7)	6.916(8)	0.7295	0.616	0.479
500	9.484(3)	6.921(4)	0.7298	0.658	0.552
600	9.488(4)	6.924(4)	0.7298	0.701	0.596
650	9.500(2)	6.928(3)	0.7292	0.828	0.652
700	9.506(5)	6.935(6)	0.7296	0.892	0.756
750	9.518(4)	6.947(4)	0.7299	1.019	0.930
800	9.526(4)	6.954(4)	0.7300	1.104	1.032
850	9.530(2)	6.959(2)	0.7302	1.146	1.104
900	9.543(4)	6.966(4)	0.7300	1.284	1.206
950	9.546(2)	6.967(2)	0.7299	1.316	1.220
1000	9.548(2)	6.972(2)	0.7302	1.337	1.293
1050	9.565(3)	6.990(3)	0.7308	1.518	1.555
1100	9.572(4)	6.996(4)	0.7309	1.592	1.642
1150	9.579(3)	7.017(3)	0.7325	1.666	1.947

Thermal lattice expansion

The thermal lattice expansion data of the hydroxyapatite single-phase powder are shown in Table 2 and Fig. 2. The a and c axial dimensions of the hydroxyapatite increased from 25 °C to 1150 °C in four stages. In the first stage, up to 400 °C, the a and c lattice parameters of hydroxyapatite gradually expanded, with the mean thermal expansion coefficients $\alpha_a = 17.2 \times 10^{-6}$ °C^{-1} and $\alpha_c = 11.0 \times 10^{-6}$ °C^{-1}. In the region from 400 °C to 600 °C, both axial dimensions expanded moderately ($\alpha_a = 4.2 \times 10^{-6}$ °C^{-1}, $\alpha_c = 5.8 \times 10^{-6}$ °C^{-1}). This non-linear expansion was attributed to the condensation of HPO_4^{2-} and to dehydration [21,30]. A weak HPO_4^{2-} IR band at 875 cm^{-1} was detected for the hydroxyapatite powder calcined at 800 °C for 3 h, while, after being heated at 600 °C for 24 h, the HPO_4^{2-} band vanished and a small $P_2O_7^{4-}$ band appeared at 730 cm^{-1}. A weight loss of 0.2% with a broad endotherm in the temperature range from 200 °C to 600 °C was observed by TG–DTA. Above 600 °C, the thermal lattice expansion increased again with the mean (600–1000 °C) coefficients $\alpha_a = 16.4 \times 10^{-6}$ °C^{-1} and $\alpha_c = 18.6 \times 10^{-6}$ °C^{-1}. At temperatures between 1000 °C and 1150 °C, the c axial expansion with $\alpha_c = 41.0 \times 10^{-6}$ °C^{-1} was remarkable and has been ascribed to the formation of oxyapatite, $Ca_{10}(PO_4)_6(OH)_{2-2x}O_x\square_x$, where $\square$ is a vacancy and $x < 1$ [17,20,33]. In the

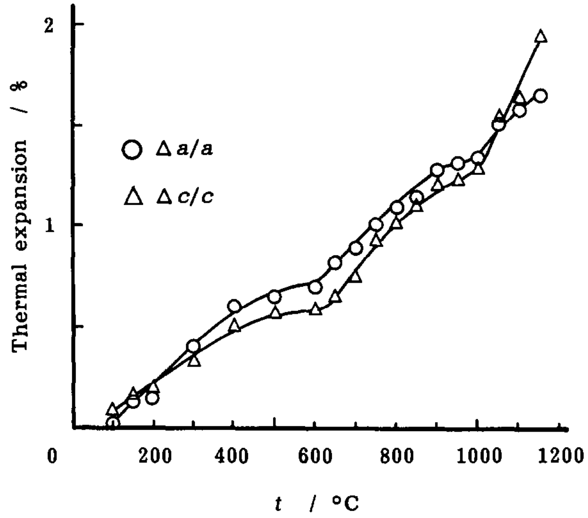

Fig. 2. Thermal lattice expansion relative to 25 °C of $\Delta a/a$ and $\Delta c/c$ of hydroxyapatite single-phase powder calcined in air at 800 °C for 1 h.

present study, the OH stretching band (3570 cm^{-1}) of the calcined hydroxyapatite powder heated at 1100 °C for 6 h in air was lower than prior to being heated.

The thermal lattice expansion data of the β-tricalcium phosphate single-phase powder are compiled in Table 3. The a and c lattice parameters of the β-tricalcium phosphate expanded linearly from 25 °C to 400 °C (Fig. 3). The mean (25–400 °C) thermal expansion coefficients of a and c were $\alpha_a = 3.9 \times 10^{-6}$ $°\text{C}^{-1}$ and $\alpha_c = 18.6 \times 10^{-6}$ $°\text{C}^{-1}$, respectively. Between 400 °C and 600 °C, the axial expansions were relatively moderate. In the upper tempera-

TABLE 3

Cell dimensions, c/a ratio and percentage expansions, relative to 25 °C, at high temperature for β-tricalcium phosphate

Temperature (°C)	a (Å)	c (Å)	c/a	$\Delta a/a$ (%)	$\Delta c/c$ (%)
25	10.446(2)	37.381(7)	3.578		
100	10.448(5)	37.43(2)	3.583	0.019	0.131
400	10.461(7)	37.64(2)	3.598	0.144	0.693
600	10.464(6)	37.63(3)	3.596	0.172	0.666
700	10.489(3)	37.92(1)	3.615	0.412	1.442
800	10.497(3)	38.04(2)	3.624	0.488	1.763
850	10.502(5)	38.13(2)	3.631	0.536	2.004
900	10.514(6)	38.08(3)	3.622	0.651	1.870
950	10.518(6)	38.00(3)	3.613	0.690	1.656
1000	10.522(5)	38.32(3)	3.642	0.728	2.512
1050	10.530(1)	38.40(1)	3.647	0.804	2.726

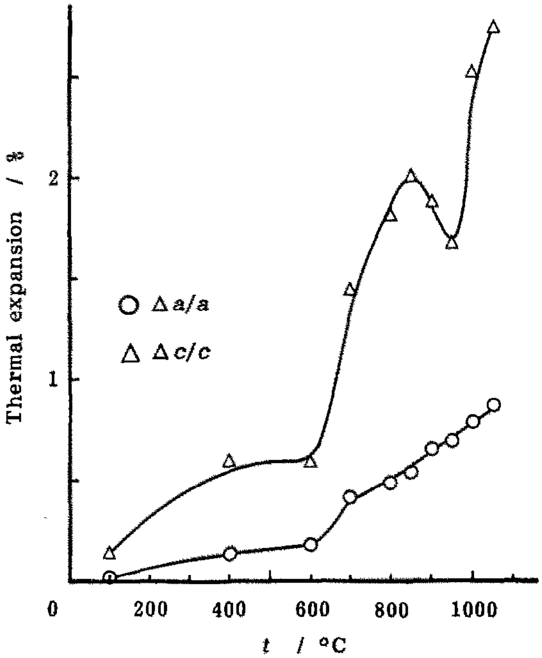

Fig. 3. Thermal lattice expansion relative to 25 °C of $\Delta a/a$ and $\Delta c/c$ of β-tricalcium phosphate single-phase powder calcined in air at 800 °C for 1 h.

ture region from 600 °C to 1050 °C, the *a* axial dimension expanded linearly with the larger mean thermal coefficient of $\alpha_a = 13.2 \times 10^{-6}$ $°C^{-1}$. From 600 °C to 850 °C, the *c* axial dimension also expanded linearly with $\alpha_c = 51.5 \times 10^{-6}$ $°C^{-1}$, and then rapidly decreased up to 950 °C: then *c* expanded again to 1050 °C. Thus, in all temperature regions, β-tricalcium phosphate has a considerably anisotropic thermal expansion coefficient.

The thermal coefficient changes at temperatures between 25 °C and 600 °C were ascribable to the formation of $P_2O_7^{4-}$ and H_2O from a very small amount of HPO_4^{2-} in the structure and the concurrent dehydration. The IR spectrum of the calcined β-tricalcium phosphate powder heated at 600 °C for 24 h contained no HPO_4^{2-} absorption band at 875 cm^{-1} but a very small $P_2O_7^{4-}$ band at 730 cm^{-1}. The X-ray powder diffraction pattern of the calcined powder heated at 600 °C was assigned to β-tricalcium phosphate and showed neither $Ca_2P_2O_7$ nor its hydrate peaks.

It was assumed that the non-linear thermal expansion of the *c* axial dimension from 850 °C to 1050 °C was attributed to the formation of an intermediate phase between the β- and α-tricalcium phosphate phases. The intermediate phase peaks were detected by the slightly lower angular positions of the (122), $(02\overline{1}0)$, (217), (128) and $(21\overline{1}0)$ β-tricalcium phosphate reflections for $20° < 2\theta < 40°$ at 950 °C, using high-temperature X-ray diffractometry (Fig. 4). These peak angles shifted lower with an increase in

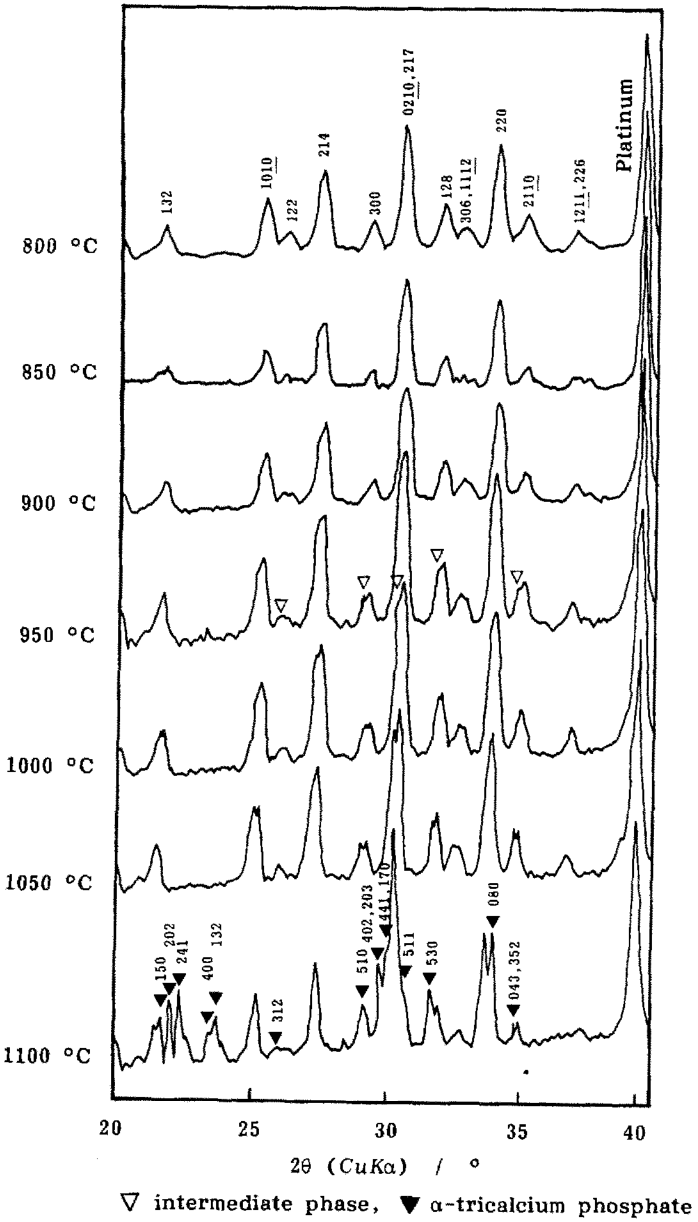

Fig. 4. X-ray powder diffraction patterns at temperatures between 850 °C and 1050 °C of β-tricalcium phosphate single-phase powder calcined in air at 800 °C for 1 h.

temperature and conformed to the (312), (510), (441), (170), (530), (043) and (352) reflections of α-tricalcium phosphate (in an orthorhombic cell) at 1150 °C. It has been reported that the intermediate phase is formed from Mg^{2+}- and H^{+}-containing β-tricalcium phosphate (whitlockite) by heating at 1000–1200 °C [32,34]. Although β-$Ca_3(PO_4)_2$ [23] has a slightly different

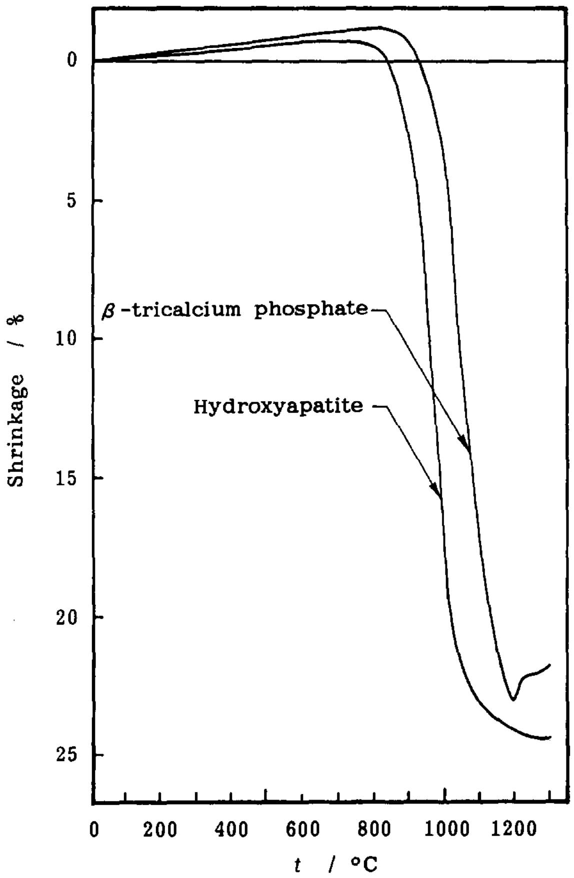

Fig. 5. Sintering shrinkage curves of hydroxyapatite and β-tricalcium phosphate pressed powder pellets at a heating rate of 5 °C $\min^{-1}$.

structure from whitlockite [32], it is reasonable to expect an intermediate phase of $Ca_3(PO_4)_2$ to exist.

Sintering shrinkage of polycrystalline ceramics

The sintering shrinkage curves of the hydroxyapatite and β-tricalcium phosphate single-phase pressed powder pellets are shown in Fig. 5. The hydroxyapatite polycrystalline ceramics expanded from room temperature to 680 °C at a rate of $12.3 \times 10^{-6}\ {}^\circ C^{-1}$. The ±0.4% non-linearity observed by high-temperature X-ray diffractometry was hardly detected. The sintering shrinkage from room temperature to 1150 °C was 23.7% in length and 55.6% in volume. This volumetric shrinkage agreed with the 55.4% shrinkage calculated from the increasing rate of the apparent relative densities measured by the weight method, 53.7% prior to sintering and 97.0% after being sintered at 1150 °C. The sintering shrinkage of the hydroxyapatite polycrystalline ceramics was apparently saturated at 1250 °C.

The β-tricalcium phosphate polycrystalline ceramics expanded on heating from room temperature to 810 °C at a rate of 16.2×10^{-6} $^\circ C^{-1}$, while they contracted above 810 °C. The non-linearity observed by high-temperature X-ray diffractometry was hardly detected. The sintering shrinkage from room temperature to 1150 °C was 21.9% in length and was equivalent to 52.4% in volume. The calculated shrinkage in volume was almost equal to 52.8%, calculated from the measured relative densities (52.1% prior to sintering, 98.6% after being sintered at 1150 °C). The sintering shrinkage reached a maximum at 1180 °C and decreased sharply. This sudden change in shrinkage behaviour was ascribed to a phase transformation from β- to α-tricalcium phosphate. The apparent expansion above 1180 °C corresponded to the decrease in calculated density from 3.03 g cm^{-3} in the

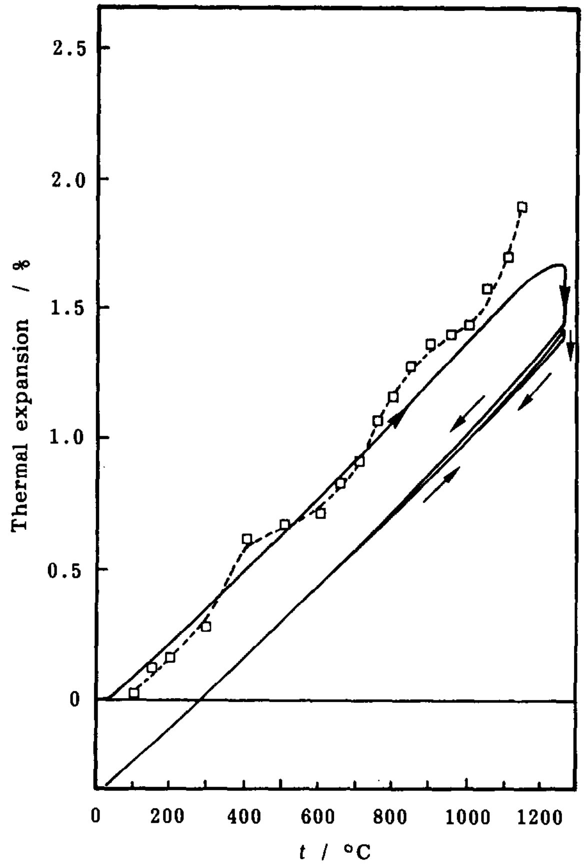

Fig. 6. Thermal expansion hysteresis curve of densely sintered hydroxyapatite ceramics at a heating rate of 5 °C min^{-1}, with plots (□) of equivalent isotropic thermal lattice expansion, $\Delta l/l$.

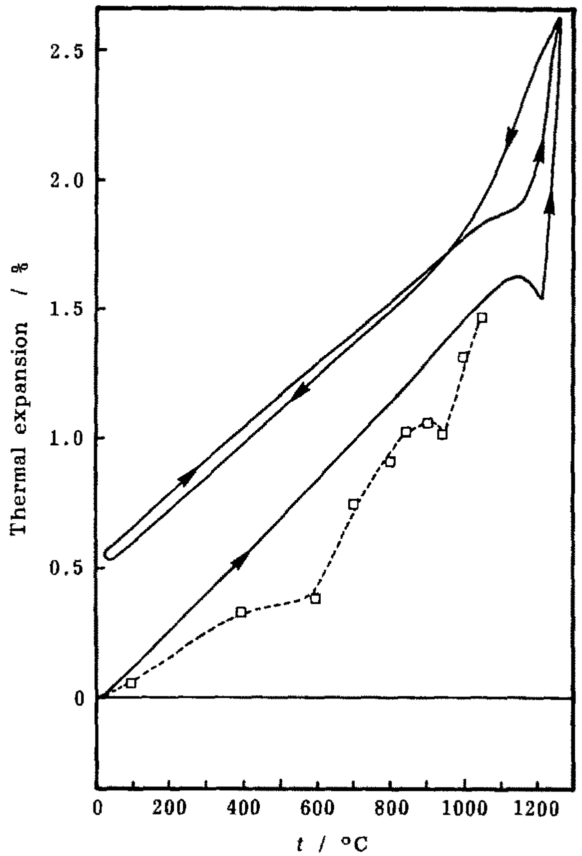

Fig. 7. Thermal expansion hysteresis curve of densely sintered β-tricalcium phosphate ceramics at a heating rate of 5 °C min^{-1}, with plots (□) of equivalent isotropic thermal lattice expansion, $\Delta l/l$.

β-form to 2.86 g cm^{-3} in the α-form. The transformation from α- to β-form occurs so late in the heating [24] that the α-phase remains at room temperature. The α-tricalcium phosphate phase was detected by X-ray diffractometry in the tricalcium phosphate ceramics sintered at 1200 °C.

Thermal expansion of polycrystalline ceramics

Thermal expansion hysteresis curves of dense hydroxyapatite and β-tricalcium phosphate sintered at 1150 °C are shown in Figs. 6 and 7. The equivalent isotropic thermal lattice expansion of $\Delta l/l$ defined by

$$\Delta l/l = \left(a^2c/a_0{}^2c_0\right)^{\frac{1}{3}} - 1 \qquad (2)$$

where a and c are the lattice parameters at the required temperature and a_0 and c_0 are the lattice parameters at 25 °C, were plotted with the hysteresis curves.

The hydroxyapatite ceramics expanded linearly up to 1150 °C with a mean (25–1150 °C) thermal expansion coefficient of 13.7×10^{-6} °C^{-1}. The expansion value reached 1.67% at 1250 °C and then decreased as the sintering reaction progressed. After one cycle of heating at 1250 °C for 1 h, the shrinkage was 0.37% in length (98.9% in relative density) and apparently saturated. The non-linearity in the temperature range from 25 °C to 1000 °C observed by high-temperature X-ray diffractometry was not detected for the samples sintered at 1150 °C.

The β-tricalcium phosphate ceramics also expanded linearly up to 1020 °C with a mean (25–1020 °C) thermal expansion coefficient of 14.9×10^{-6} °C^{-1}. Although the ceramics shrank in the temperature range from 1020 °C to 1180 °C, they sharply expanded above 1180 °C. The non-linearity (25–800 °C) of the β-tricalcium phosphate observed by X-ray diffractometry was not detected. The shrinkage in the temperature region from 1020 °C to 1180 °C was ascribed to formation of the intermediate phase as mentioned above. The higher (approx. 100 °C) temperature of the shrinkage measured by thermomechanical analysis (TMA), compared with high-temperature X-ray diffractometry, was attributed to the higher actual heating rate in TMA. The rapid thermal expansion over 1080 °C was due to α-phase formation and reached 2.26% after heating at 1250 °C for 1 h. After one cycle of heating, a thermal expansion of 0.56% remained at 25 °C. This residual expansion was ascribable to the α-tricalcium phosphate remaining at room temperature. From the transmission electron micrograph (Fig. 8), it is assumed that the α-phase produced strain in the ceramic grains.

Fig. 8. Transmission electron micrograph of β-tricalcium phosphate ceramics sintered at 1150 °C.

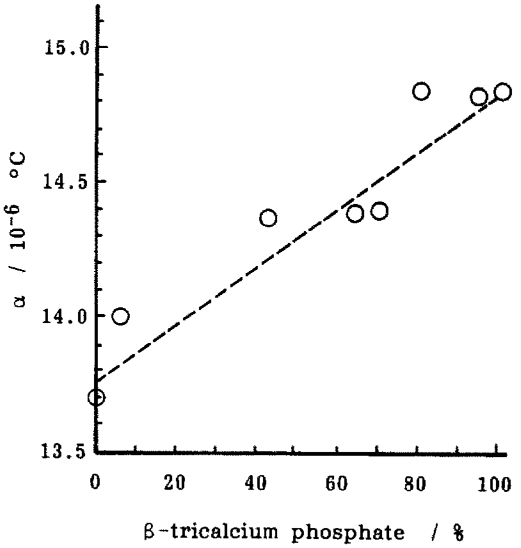

Fig. 9. Mean (25–1000 °C) thermal expansion coefficient of densely sintered hydroxyapatite–β-tricalcium phosphate ceramics in relation to β-tricalcium phosphate content.

The mean (25–1000 °C) thermal expansion coefficient of the hydroxyapatite–β-tricalcium phosphate ceramics sintered at 1150 °C for 1 h with respect to the β-tricalcium phosphate content is shown in Fig. 9. The thermal coefficient increased almost linearly with an increase in β-tricalcium phosphate content.

CONCLUSIONS

Hydroxyapatite and β-tricalcium phosphate prepared by the wet method exhibit non-linear thermal lattice expansion as revealed by high-temperature X-ray powder diffractometry. The non-linear thermal expansion of both hydroxyapatite and β-tricalcium phosphate single-phase powder at temperatures between 25 °C and 600 °C was attributed to the condensation of structural HPO_4^{2-} and dehydration. In the upper temperature region, the hydroxyapatite c axial dimension sharply expanded in the temperature range from 1000 to 1150 °C owing to the formation of oxyapatite, $Ca_{10}(PO_4)_6\text{-}(OH)_{2-2x}O_x\square_x$, where $\square$ = vacancy and $x < 1$. The c axial dimension of the β-tricalcium phosphate shrank in the range from 850 °C to 950 °C. This drastic shrinkage was ascribed to the formation of an intermediate phase between the β- and α-tricalcium phosphate phases.

The densely sintered hydroxyapatite–β-tricalcium phosphate ceramics possessed thermal expansion hysteresis, as observed by thermomechanical analysis (TMA). The non-linear thermal expansion of both hydroxyapatite and β-tricalcium phosphate in the temperature range from 25 ° C to 600 ° C was not detected by TMA. The shrinkage of the β-tricalcium phosphate due to formation of the intermediate phase was observed, remarkably, at a temperature between 1020 ° C and 1180 ° C. A sharp thermal expansion above 1180 ° C due to α-phase formation was also observed.

The mean (25–1000 ° C) thermal expansion coefficient of the densely sintered hydroxyapatite–β-tricalcium phosphate ceramics increased almost linearly with an increase in β-tricalcium phosphate content. This linear increase suggested that the thermal expansion coefficient of the hydroxyapatite–β-tricalcium phosphate plasma-spray-coated layer could be adjusted to the coefficient of the metals used as the base. The complex thermal expansion of hydroxyapatite–β-tricalcium phosphate ceramics is a problem that demands careful consideration in order to improve the bonding strength of the plasma spray coating interfaces.

ACKNOWLEDGEMENTS

The author would like to thank Dr. Y. Suyama and Dr. K. Suzuki, Japan Fine Ceramics Centre, for use of their high-temperature X-ray powder diffractometer. We are deeply indebted to Dr. H. Ikawa, Tokyo Institute of Technology, for his invaluable suggestions.

REFERENCES

1 K. Kato, H. Aoki, T. Tabata and M. Ogiso, Biomat. Med. Dev. Art. Org., 7 (1979) 291.
2 H.W. Denisson, K. de Groot, P.Ch. Makkes, A. van den Hoof and R.J. Klopper, J. Biomed. Mater. Res., 14 (1980) 713.
3 H. Aoki, K. Kato and T. Tabata, Report of the Institute for Medical and Dental Engineering, Tokyo Medical and Dental University, 11 (1977) 33.
4 G. Riess, International Congress of Implantology and Biomaterials in Stomatology, Kyoto, 1980, p. 92.
5 H. Aoki, Y. Shin, M. Akao and R. Kikuchi, Jpn. J. Artif. Organs, 13 (1984) 1131.
6 M. Jarcho, R.L. Salsbury, M.B. Thomas and R.H. Doremus, J. Mater. Sci., 14 (1979) 142.
7 M. Akao, H. Aoki and K. Kato, J. Mater. Sci., 16 (1981) 809.
8 M. Akao, H. Aoki, K. Kato and A. Sato, J. Mater. Sci., 17 (1982) 343.
9 M. Akao, N. Miura and H. Aoki, Yogyo-Kyokai-Shi, 92 (1984) 672.
10 K. Okano, T. Fukubayasi, S. Tomobe, A. Ohno, O. Uematu, M. Fukui, T. Tateishi and Y. Shirasaki, Ceramic Implants, Vol. 4, Japanese Society of Orthopaedic Ceramic Implants, 1984, pp. 187–192.
11 K. de Groot, R. Geesink, C.P.A.T. Klein and P. Serekia, J. Biomed. Mater. Res., 21 (1987) 1375.
12 R. Geesink, K. de Groot and C.P.A.T. Klein, J. Bone Joint Surg., 70B (1988) 17.
13 O.R. Trautz, Ann. NY Acad. Sci., 60 (1955) 696.
14 A.S. Posner, A. Perloff and A.F. Diorio, Acta Crystallogr., 11 (1958) 308.
15 R.A. Young and J.C. Elliott, Arch. Oral Biology, 11 (1966) 699.

16 P.E. Macie, J.C. Elliott and R.A. Young, Acta Crystallogr., B28 (1972) 1840.
17 J.C. Trombe and G. Montel, J. Inorg. Nucl. Chem., 40 (1978) 15.
18 J. Arends, J. Schuthof, W.H. van der Linden, P. Bennea and P.J. van den Berg, J. Cryst. Growth, 46 (1979) 213.
19 R.M.H. Verbeeck, H.J.M. Heilligers, F.C.M. Driessens and H.G. Schaeken, Z. Anorg. Allg. Chem., 466 (1980) 76.
20 G.R. Fischer, P. Bardhan and J.E. Geiger, J. Mater. Sci. Lett., 2 (1983) 577.
21 W.G. Perdok, J. Christoffersen and J. Arends, J. Cryst. Growth, 80 (1987) 149.
22 D. Taylor, Br. Ceram. Trans. J., 87 (1988) 88.
23 B. Dickens, L.W. Schroeder and W.E. Brown, J. Solid State Chem., 10 (1974) 232.
24 H. Monma and M. Goto, Yogyo-Kyokai-Shi, 91 (1983) 473.
25 J. Murphy and J.P. Riley, Anal. Chim. Acta, 27 (1962) 31.
26 T. Sakurai (Ed.), UNICS (Universal Crystallographic Computation System), The Crystallographic Society of Japan, 1967.
27 Y.S. Touloukian, R.K. Kirby, R.E. Taylor and T.Y.R. Leep (Eds.), Thermophysical Properties of Matter, Thermal Expansion, Vol. 13, IFI/Plenum Press, 1977, p. 176.
28 G. Montel, Ann. Chim., 4 (1969) 255.
29 S.J. Joris and C.H. Amberg, J. Phys. Chem., 75 (1971) 3167.
30 R.A. Young and D.W. Holcomb, Calcif. Tissue Int., 36 (1984) 60.
31 R.A. Terpstra, F.C.M. Driessens, H.G. Schaeken and R.M.H. Verbeeck, Z. Anorg. Allg. Chem., 507 (1983) 206.
32 R. Gopal, C. Calvo, J. Ito and W.K. Sabine, Can. J. Chem., 52 (1974) 1155.
33 T. Kijima and M. Tsutsumi, J. Am. Ceram. Soc., 62 (1979) 455.
34 R. Gopal and C. Calvo, Nature Phys. Sci., 237 (1972) 30.